Received: 2 January 2020 | Revised: 12 June 2020 | Accepted: 16 June 2020

DOI: 10.1002/jnr.24690

RESEARCH ARTICLE

Impact of network-targeted multichannel transcranial direct current stimulation on intrinsic and network-to-network functional connectivity

Lucia Mencarelli[1] | Arianna Menardi[1] | Francesco Neri[1] | Lucia Monti[2] | Giulio Ruffini[3,4] | Ricardo Salvador[3,4] | Alvaro Pascual-Leone[5] | Davide Momi[1] | Giulia Sprugnoli[1] | Alessandro Rossi[1,6] | Simone Rossi[1,6] | Emiliano Santarnecchi[1,5]

[1]Siena Brain Investigation & Neuromodulation Lab (Si-BIN Lab), Department of Medicine, Surgery and Neuroscience of the Siena School of Medicine, Neurology and Clinical Neurophysiology Section, University of Siena, Siena, Italy

[2]Unit of Neuroimaging and Neurointervention, "Santa Maria alle Scotte" Medical Center, Siena, Italy

[3]Neuroelectrics, Cambridge, MA, USA

[4]Neuroelectrics, Barcelona, Spain

[5]Berenson-Allen Center for Non-Invasive Brain Stimulation, Beth Israel Deaconess Medical Center, Harvard Medical School, Boston, MA, USA

[6]Human Physiology Section, Department of Medicine, Surgery and Neuroscience, University of Siena, Siena, Italy

Correspondence
Emiliano Santarnecchi, Berenson-Allen Center for Non-Invasive Brain Stimulation, Beth Israel Deaconess Medical Center, Harvard Medical School, Boston, MA, USA.
Email: esantarn@bidmc.harvard.edu

Funding information
National Institutes of Health, Grant/Award Number: R01 AG060981-01

Abstract

Dynamics within and between functional resting-state networks have a crucial role in determining both healthy and pathological brain functioning in humans. The possibility to noninvasively interact and selectively modulate the activity of networks would open to relevant applications in neuroscience. Here we tested a novel approach for multichannel, network-targeted transcranial direct current stimulation (net-tDCS), optimized to increase excitability of the sensorimotor network (SMN) while inducing cathodal inhibitory modulation over prefrontal and parietal brain regions negatively correlated with the SMN. Using an MRI-compatible multichannel transcranial electrical stimulation (tES) device, 20 healthy participants underwent real and sham tDCS while at rest in the MRI scanner. Changes in functional connectivity (FC) during and after stimulation were evaluated, looking at the intrinsic FC of the SMN and the strength of the negative connectivity between SMN and the rest of the brain. Standard, bifocal tDCS targeting left motor cortex (electrode ~C3) and right frontopolar (~Fp2) regions was tested as a control condition in a separate sample of healthy subjects to investigate network specificity of multichannel stimulation effects. Net-tDCS induced greater FC increase over the SMN compared to bifocal tDCS, during and after stimulation. Moreover, exploratory analysis of the impact of net-tDCS on negatively correlated networks showed an increase in the negative connectivity between SMN and prefrontal/parietal areas targeted by cathodal stimulation both during and after real net-tDCS. Results suggest preliminary evidence of the possibility of manipulating distributed network connectivity patterns through net-tDCS, with potential relevance for the development of cognitive enhancement and therapeutic tES solutions.

KEYWORDS
brain networks, brain stimulation, fMRI, functional connectivity, tDCS, tES

Edited by Jeremy Hogeveen. Reviewed by Rany Abend and Alberto Pisoni.

1 | INTRODUCTION

Transcranial direct current stimulation (tDCS) is a noninvasive brain stimulation (NIBS) technique capable of influencing spontaneous neuronal activity by increasing or decreasing the average resting membrane potential of neuronal populations underneath, respectively, positively (i.e., anode) and negatively (cathode) charged scalp electrodes (Paulus, 2003) (Nitsche & Paulus, 2001). For instance, when applied to the motor system, tDCS has been found to increase corticomotor excitability—up to 90 min following stimulation (Nitsche & Paulus, 2001)—and to enhance motor performance in healthy individuals—up to 45 min after stimulation's cessation (van Asseldonk & Boonstra, 2016)—possibly acting on cortical plasticity mechanisms (Antal, Terney, Poreisz, & Paulus, 2007; Boros, Poreisz, Münchau, Paulus, & Nitsche, 2008; Fritsch et al., 2010; Furubayashi et al., 2008; Nitsche & Paulus, 2000; Nitsche et al., 2005; Uy, Ridding, Hillier, Thompson, & Miles, 2003). Moreover, results from studies on clinical populations with motor deficits suggest tDCS as a promising neuromodulatory tool to restore motor function (Liew, Santarnecchi, Buch, & Cohen, 2014) (for a review see Sánchez-Kuhn, Pérez-Fernández, Cánovas, Flores, & Sánchez-Santed, 2017).

Local- and network-level changes related to anodal and cathodal tDCS have been already helping the development of ad-hoc research designs (Pellicciari, Brignani, & Miniussi, 2013; Pisoni et al., 2018; Romero Lauro et al., 2014; Varoli et al., 2018). However, traditional tDCS research employs a two-electrode montage with rather large rectangular electrodes. The poor focality and the risk of producing diffuse electric fields in the brain—which could exert unspecific cortical effects—represent a known downfall of tDCS (Miranda, Mekonnen, Salvador, & Ruffini, 2013). Moreover, brain regions do not operate in isolation, but rather continuously interact with each other in well-organized cortical networks (Fischer et al., 2017; Fox et al., 2005; Sheffield & Barch, 2016), creating the need for tDCS solutions able to target brain networks. This becomes even more important when considering how alteration of such networks are also responsible for psychological and neurological deficits in almost any neurological or psychiatric condition (Drysdale et al., 2017; Fox, 2018; Fox, Buckner, White, Greicius, & Pascual-Leone, 2012; Sheffield & Barch, 2016).

Therefore, if brain networks are becoming the targets of neuromodulatory interventions, stimulation of a single brain region might no longer be sufficient. Our group (Fischer et al., 2017) has recently tested a novel approach for multifocal network-targeted tDCS (net-tDCS) of the primary motor cortex (M1) and its associated resting-state fMRI network. The approach is based on a genetic algorithm to produce cortical electric fields optimally matched to a desired characteristic of a cortical map obtained from, for example, individual fMRI, PET, or EEG data (Ruffini et al., 2014). The algorithm explores a large, combinatorial parameter space, including current intensity, number and location of electrodes, and stimulation polarity, resulting in the best optimization to maximize injection of current in the target region/network while minimizing stimulation of the rest of the brain. By optimizing the net-tDCS solution on the basis of a resting-state functional connectivity (FC) map of the right hand representation on the left motor cortex, we investigated the impact of network-targeted tDCS on corticospinal excitability via combined Transcranial Magnetic Stimulation (TMS) and electromyography (EMG). Net-tDCS induced approximately two times the increase in left M1 excitability over time (compared to traditional bifocal tDCS targeting left M1 and contralateral fronto-orbital region), with a concomitant increase in the excitability of the contralateral motor cortex (usually not induced by traditional tDCS applied solely over left M1). Results suggested the possibility of using network-targeted stimulation approaches to engage multiple nodes of a given network, possibly resulting in an overall greater modulatory effect (Ruffini et al., 2018). However, TMS-tDCS measurements do not entail the same specificity in assessing network-level changes compared to that can be achieved with combined tDCS-fMRI (Antal, Polania, Schmidt-Samoa, Dechent, & Paulus, 2011; Lindenberg, Nachtigall, Meinzer, Sieg, & Floel, 2013; Meinzer et al., 2012; Meinzer, Lindenberg, Antonenko, Flaisch, & Flöel, 2013; Polanía, Nitsche, & Paulus, 2011; Zheng, Alsop, & Schlaug, 2011). Among the major advantages, simultaneous tDCS-fMRI allows to produce whole-brain data at high spatial resolution, uncovering changes in brain activity over both stimulated and not-stimulated region(s). Moreover, this allows to also look at changes in network-to-network dynamics, a relevant target for net-tDCS.

Here we attempted to replicate the findings previously reported by Fischer et al. (2017) by directly looking at changes in network dynamics during a concurrent tDCS-fMRI study. In particular, we tested the effects of net-tDCS on the activity of (i) a target resting-state fMRI network (i.e., the sensorimotor network, SMN), as well as (ii) on its negatively correlated regions in the prefrontal and parietal lobe. To do so, we collected resting-state FC BOLD MRI (rs-FCMRI) in two groups of 10 healthy participants before, during, and after tDCS using an MRI-compatible brain stimulation device. In the first group, a canonical bifocal sponge-based tDCS targeting the left motor cortex was used. In the second group, the tDCS electrode placement was optimized to match the rs-FCMRI pattern of the right hand representation in the left motor cortex (M1), with anodal stimulation affecting

Significance

By means of electric or magnetic stimulation over a selected brain area, noninvasive brain stimulation techniques can modify brainS activity inducing long-lasting effects and even behavioral changes. However, the human brain is organized in functional networks composed by multiple regions, therefore brain stimulations solution allowing to modulate network activity as a whole are needed. Here we provide evidence of the efficacy of network-targeted electrical stimulation, showing an increase of spontaneous activity in the targeted network, as well as signs of a modulation of its interplay with other brain networks. Findings are relevant for reserch on the optimization of brain stimulation solutions in clinical populations where alteration of network connectivity rather than single brain areas have been documented, as well as for cognitive enhancement purposes.

bilateral motor cortices and cathodal stimulation eliciting maximal inhibition over prefrontal and parietal cortices as in Fischer et al. (2017) (see Figure 1). By comparing the increase in FC over the SMN between these two groups we want to verify whether stimulating only one motor cortex (left) or the entire SMN would lead to different changes in FC. In particular, we hypothesized that (i) net-tDCS would elicit a stronger modulation of the SMN as a whole, that is, a greater change in FC of both left/right motor cortices during as well as after stimulation compared to standard tDCS (which should selectively modulate only the left motor cortex, as previously found in Fischer et al., 2017). Moreover, in order to validate potential effect of net-tDCS over network-to-network dynamics, we compared the effect induced by real and sham net-tDCS on negative FC. In particular, we assumed that (ii) net-tDCS would also modulate the FC between SMN and its negatively correlated regions (resembling the frontoparietal network, FPN; Corbetta, 1998). Finally, given the different number and distribution of electrodes on the scalp for net-tDCS and bifocal tDCS, side/adverse effects and subjective feelings during both stimulation approaches were assessed after each session.

2 | MATERIALS AND METHODS

2.1 | Participants

Two groups of 10 right-handed healthy individuals (14 males and 6 females, age 26.3 ± 3.1), with normal neurological exam and no history of psychiatric disorders were recruited through flyers and online advertisement. Subjects with personal and family history of epilepsy were excluded, as well as those reporting recent migraine attacks. Each subject provided written informed consent. The study was approved by the Local Ethics Committee at Le Scotte Hospital and University of Siena School of Medicine (Siena, Italy; IRB protocol "APOLLO").

2.2 | Experimental paradigm

The subjects took part into two different experimental protocols: standard tDCS (eight males and two females, age 25.5 ± 3.5) and network-targeted tDCS (net-tDCS hereafter; six males and four females, age 27.2 ± 2.5). Each condition consisted of two randomized experimental sessions, real-tDCS and shamtDCS, held on separated days at least 1 week apart. Four resting-state fMRI were acquired in order to evaluate brain FC at different time point: before, during, and after tDCS. In particular, the first resting state scan was computed as a baseline without the stimulation, the second and the third fMRI were computed concurrent to tDCS to evaluate "acute" and "cumulative" stimulation effects, whereas the last one was used for evaluating tDCS after-effect. The experimental design is shown in Figure 1a. The duration of the experiment was approximately 1 hr per session. At the end of each study visit, a questionnaire evaluating possible side effects of stimulation was administered (Fertonani, Rosini, Cotelli, Rossini, & Miniussi, 2010).

2.3 | Brain stimulation device

tDCS was delivered by means of an MRI-compatible Starstim hybrid EEG/tCS eight-channel neurostimulator system (Neuroelectrics, Barcelona, Spain). The device was connected via Bluetooth to a computer located outside the Faraday cage (Figure 1b). The stimulation protocol was created and monitored using the NIC 2.0 software (www.neuroelectrics.com/products/software/nic2/). MR-compatible electrodes consisting of conductive rubber electrodes were used (Figure 1b) and inserted in circular sponge sockets soaked with 15 ml of sterile sodium chloride solution (0.9%) for at least 10 min (MRI Sponstim, Neuroelectrics). The electrodes were positioned in a neoprene cap with 32 electrode positions corresponding to the 10/20 EEG system. The stimulator was connected to the MR-compatible electrodes by specially designed MR-compatible (nonferrous and radio translucent) leads.

2.4 | Standard tDCS protocol

Traditional tDCS was applied using a "standard" montage widely used in the tDCS literature (Lefaucheur et al., 2017), with the anode over the left M1 area (C3 in the 10/20 EEG-reference system) and the cathode over the right supraorbital area (Fp2; Figure 1d). A current intensity equal to 2mA was delivered by means of 23-cm^2 round electrodes positioned inside saline-soaked sponges (25 cm^2 contact area, Figure 1b). This montage is thought of activating the motor system with a major focus on the left motor cortex. Given the nature of bifocal tDCS, a second electrode delivering cathodal stimulation needs to be placed on the scalp. In the case of bifocal tDCS for motor cortex stimulation, the cathode is usually placed over a "neutral" region (i.e., contralateral frontopolar region, Fp2), which implies the potential induction of two stimulation effects: a desired anodal –excitatory– stimulation over M1, and an unspecific cathodal –inhibitory– stimulation over the right frontopolar cortex, both potentially contributing to resulting changes in brain physiology and/or behavior. Net-tDCS was thought of leveraging such limitation of canonical tDCS by systematically placing anodes and cathodes following fMRI-based patterns of positive and negative connectivity within/outside the motor system. This should lead to both a stronger modulation of motor system's excitability compared to standard tDCS, as well as to the modulation of functionally relevant network-to-network dynamics between motor cortices and the rest of the brain via carefully tailored cathodal stimulation (see below).

2.5 | Network-targeted tDCS optimization

As in Fischer et al. (2017), the target region for net-tDCS was based on the hand area representation of the left motor cortex (Figure 1c). The FC pattern of the hand area was calculated (Figure 1c); the coordinates of five largest clusters positively correlated with left M1 are: $x = -42$, $y = -18$, $z = 62$; $x = 50$, $y = -72$, $z = 2$; $x = 18$, $y = -82$,

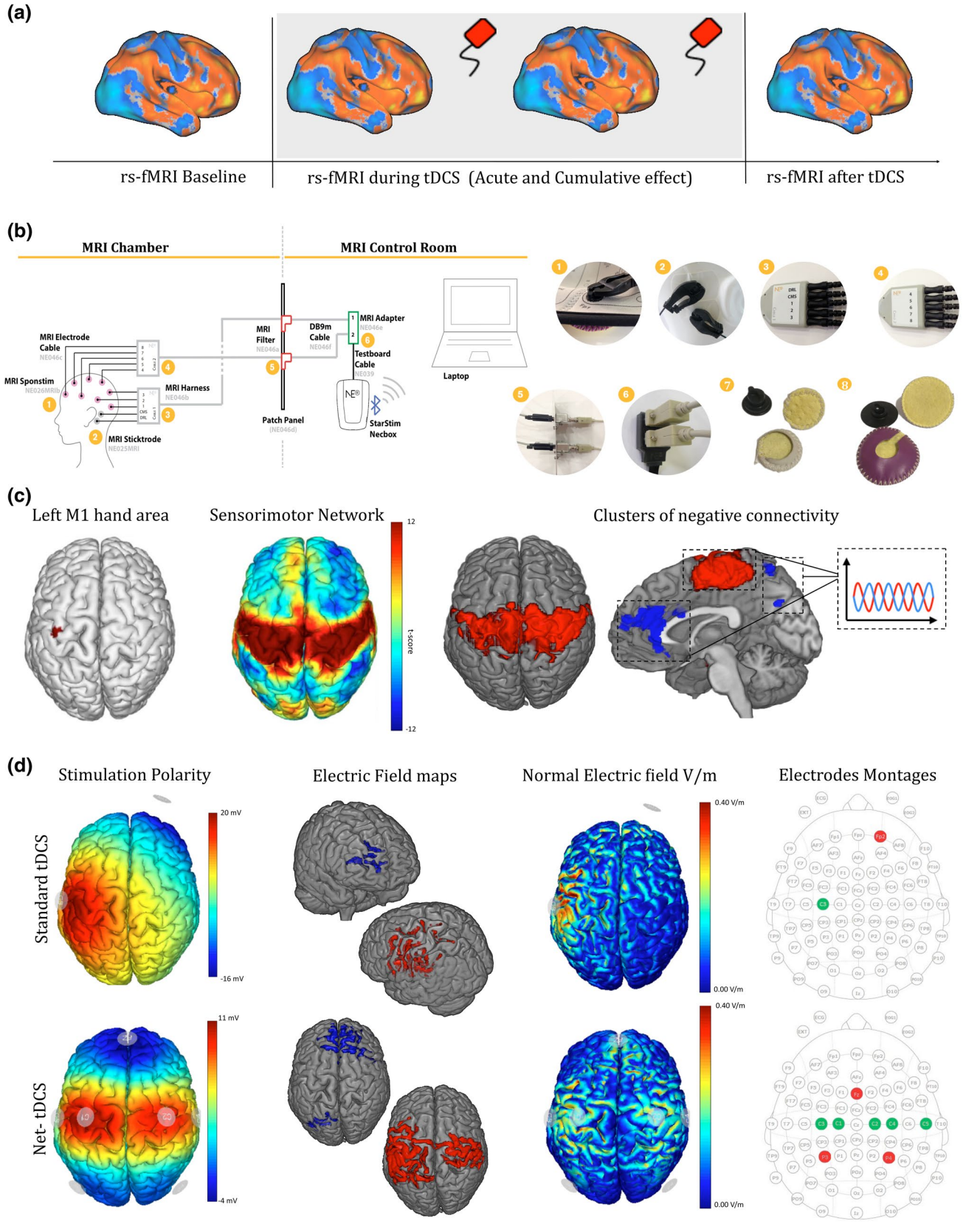

$z = 30$; $x = -10$, $y = -88$, $z = 36$; $x = -50$, $y = -74$, $z = 8$; whereas the coordinates of five largest clusters negatively correlated with left M1 are: $x = 46$, $y = -46$, $z = 40$; $x = -40$, $y = 24$, $z = 32$; $x = -8$, $y = -78$, $z = -26$; $x = -30$, $y = 18$, $z = -6$; $x = -54$, $y = -54$, $z = -4$. This pattern was used as input for the optimization of a genetic algorithm (Stimweaver algorithm; Ruffini et al., 2014) comparing thousands

FIGURE 1 Experimental paradigm. (a) Overview of the tDCS-fMRI experimental session. (b) Schematic of multichannel stimulator MRI installation (system supplied by neuroelectrics.com). (1) electrode in cap detail, (2) Common Mode Sense (CMS) active and Driven Right Leg (DRL) passive mastoid electrodes for impedance check, (3) and (4) MRI-compatible touchproof connector, (5) Patch panel connection, (6) Starstim cable adaptor, MRI-compatible rubber electrodes used for (7) standard (5 × 5 cm) and (8) net-tDCS (1 cm radius circular electrodes) . (c) The hand area of left M1 (targeted by standard tDCS) and areas positively and negatively connected to left M1, constituting the sensorimotor resting-state network (targeted by net-tDCS) are reported. Clusters of negative connectivity to the SMN are shown. (d) For both standard and net-tDCS stimulation polarity, electric field maps >0.25 V/m (red = anodal, blue = cathodal), normal electric field, and electrode positions (right; green anodes, red cathodes) are shown [Color figure can be viewed at wileyonlinelibrary.com]

of multi-electrode montages including up to eight stimulating electrodes located on any of the 32 positions of the 10/20 International EEG system. The goal of maximizing excitation or inhibition of the target regions was mathematically implemented by the rationale that an inward (outward) electric field component normal to the cortical surface (E_n) excites (or inhibits) the underlying cortical pyramidal cells (this is the so-called "lambda-E" model, see Ruffini et al. (2013) and references therein). Solutions were found using constrained least squares minimization to determine the electrode positions and currents that induced a weighted E_n field that best approximated the weighted target (i.e., the weighting of the FC values in the map). The desired E_n field component was set to 0.25 V/m (the positive value indicates that the target E_n field is directed into the cortical surface, thus having an excitatory effect) in the target area. Stimulation was performed using MRI-compatible Sponstim electrodes (circular 1-cm radius, π cm^2 area sponges, Neuroelectrics), with a maximal current at any electrode of 2.0 mA, and a maximal total injected current of 4.0 mA across eight electrodes (Figure 1d). Stimulation parameters were maintained within recommended safety parameters for transcranial electrical stimulation (tES) in humans (Lefaucheur et al., 2017). Anodal stimulation was delivered via five electrodes placed over the sensorimotor cortex bilaterally: specifically C1 (872 μA), C2 (888 μA), C3 (1,135 μA), C4 (922 μA), T8 (183 μA);—cathodal electrodes were placed over frontopolar and parietal areas, specifically Fz (−1,843 μA), P3 (−1,121 μA), P4 (−1,036 μA; Figure 1d).

Real-tDCS for both conditions was delivered for 22 min, with periods of ramp-up/down of 30 s, whereas sham tDCS consisted of only 60 s of stimulation at the beginning (ramp-up) and at the end (ramp-down) of the session. The impedance levels were kept below 10 kΩ throughout the stimulation sessions, thereby minimizing cutaneous sensations.

2.6 | Biophysical modeling

Two separate models were built, for standard and net-tDCS, respectively. Distribution of current and normal components of the generated electrical fields is reported for each montage in Figure 1 (C-D, for more details see Figure S1). A realistic head model based on T1-weighted and proton density (PD)-weighted MRI images of the single-subject template Colin27 was used to simulate the electric field distribution as previously described (Miranda et al., 2013). Five different tissue types were distinguished. Isotropic conductivities were used as follows: 0.33 Siemens per meter (S/m) for the scalp , 0.008 S/m for the skull, 1.79 S/m for the cerebrospinal fluid (CSF; including the ventricles), 0.4 S/m for the grey matter (GM) and 0.15 S/m for the white matter (WM). The plugs at the apexes of the orbits were given conductivity values equal to those of the scalp. In order to represent the conductivity of sponge electrodes soaked in saline solution, the electrodes were modeled with a high conductivity value of 2 S/m. The resulting voxel-level volumes were thresholded and used to define seed regions for FC MRI analysis (see dedicated paragraph).

2.7 | MRI data acquisition

Imaging was conducted on a Siemens Avanto scanner with a 12-channel head-coil (Siemens, USA). High-resolution T1-weighted anatomical images were obtained using a 3D-MPRAGE sequence (repetition time (TR) = 1,880 ms, echo time (TE) = 3.38 ms, inverse time (TI) = 1,100 ms, flip angle (FA) = 15°, number of slices = 176, thickness = 1 mm, gap = 0 mm, imaging matrix = 256 × 256, acquisition duration: 5 min). Functional MRI data were acquired before tDCS ("BASELINE"), during stimulation (mins 1′–8′ of stimulation, "ACUTE"; mins 15′–22′ of stimulation, "CUMULATIVE"), and after stimulation ("AFTER"). Functional MRI images were acquire using standard echo-planar blood oxygenation level-dependent (BOLD) imaging (TR = 2,000 ms, TE = 20 ms, flip angle (FA) = 70°, number of slices = 37, thickness = 3.59 mm, gap = 4.64 mm, acquisition duration: 8,36″). Subjects were instructed not to focus their thoughts on any particular topic, do not cross their arms or legs and keep their eyes open. Arterial spin labeling (ASL) data were also acquired before and during tDCS; however, perfusion-related results are not discussed as part of the present manuscript.

2.8 | fMRI data preprocessing

fMRI data preprocessing and statistical analyses were carried out using SPM12 software (Statistical Parametric Mapping; www.fil.ion.ucl.ac.uk/spm/) and MATLAB 2013b (MathWorks, MA, USA) software. BOLD images underwent the following preprocessing steps: discarding of the first three volumes to allow for steady-state magnetization and stabilization of participant status; slice timing; realigning to correct for head motion; co-registration to structural images; segmentation; nonlinear normalization to the Montreal Neurological Institute (MNI) template brain; voxel resampling to an isotropic 3 × 3 × 3 mm voxel size; smoothing with an isotropic Gaussian kernel (full-width at half maximum, 8 mm). Structural images were co-registered to the mean volume of functional images and segmented using routines in SPM12. To obtain a more accurate spatial normalization, we created a customized grey matter template

from all subjects' segmented images. Briefly, this approach is based on the creation of a customized anatomical template built directly from participants T1-weighted images instead of the canonical one(s) provided by SPM (MNI template, ICBM 152, MNI). This allows a finer normalization into standard space and consequently avoids under- or overestimation of brain region volume. Linear trends were removed to reduce the influence of the rising temperature of the MRI scanner and all functional volumes were bandpass filtered at 0.01 Hz < f < 0.08 Hz to reduce low-frequency drifts. Finally, an important issue for brain connectivity analysis is related to the deconvolution of potential confounding signals—mainly physiological high-frequency respiratory and cardiac noise—from the grey matter voxels' BOLD time course. We decided to regress out potential confounding signals, like physiological high-frequency respiratory and cardiac noise, from grey matter voxels' BOLD time course using the Compcorr algorithm (Whitfield-Gabrieli & Nieto-Castanon, 2012), in order to reduce artificial negative correlation and provide adequate filtering of the data.

2.9 | Second-level analysis

Given the rationale of the study, changes in FC were expected on both left and right sensorimotor cortices, as well as on their negatively correlated regions during/after net-tDCS; instead, standard tDCS was expected to induce changes only on left sensorimotor cortices and right frontopolar regions. However, the two approaches generate electric fields of different intensity, shape and polarity on the cortex, making it difficult to capture stimulation effects by implementing a single set of regions of interest (ROIs) defined anatomically. Therefore, we extracted individual resting-state networks (RSNs) for each participant using independent component analysis (ICA; Beckmann & Smith, 2005). Fifteen components were obtained from subjects' resting data and visually inspected by three investigators (LM, AM, and ES; Figure S2 shows the ICA component for the most representative RSNs). The SMN was chosen as seed to directly compare the effects of standard and network-targeted stimulation at whole-brain level. Additionally, the effect of tDCS in modulating the interaction between sensorimotor cortices and brain regions showing the highest negative FC was also investigated (Figure 1c). Specifically, these regions corresponded to a cluster of voxels mapping onto the anterior portion of the cingulate cortex (ACC hereafter) and the precuneus. In summary, FC analyses were focused on evaluating changes in local connectivity involving the sensorimotor cortices due to anodal stimulation, as well as changes in the negative connectivity between sensorimotor cortices and ACC/precuneus as a measure of network-to-network connectivity.

2.10 | FC analysis

In order to verify our hypothesis, we implemented two different analysis. The first one aimed to compare the modulation of FC induced by bifocal or net-tDCS at whole-brain level considering the SMN identified via ICA as a seed region. The second one aimed at investigating the potential network effects of net-tDCS by looking at changes in connectivity between the motor system and its negatively correlated brain regions.

2.10.1 | Whole-brain FC modulation

Statistical analysis was carried out using the CONN (v.17f) toolbox and Matlab 2013b software (Mathworks, MA, USA). A repeated measure analyses of variance (rp-ANOVA) was carried out on the connectivity profile of the SMN identified via ICA. The model included factors "Montage" (standard bifocal, network-targeted), "Condition" (real, sham), and "Time" (Baseline, Acute, Cumulative, and After tDCS), as well as "Montage × Condition × Time" interaction term. Age, gender, and order of stimulation were included as covariates in all analyses. Results were computed applying a voxel-level threshold (p < 0.001 uncorrected) and cluster size correction (p < 0.05, false discovery rate (FDR) corrected).

2.10.2 | Changes in network-to-network connectivity

To specifically investigate the effect of net-tDCS on network-to-network connectivity patterns involving the SMN, the following analysis was carried out separately for each montage (bifocal or net-tDCS) and was focused on the effects of the tCS condition (real and sham) on negative correlation/connectivity at different time points (acute, cumulative, and after tDCS). Since the standard bifocal montage was not optimized to target negatively connected nodes, we did not expect any significant effect (results related to bifocal tCS are reported as part of the supplementary material, see Figure S3).

We initially run an ICA to define the SMN across subjects (data-driven, based on our sample) and then we identified the clusters of voxels showing a significant negative connectivity with the sensorimotor ICA component at baseline (p < 0.001 uncorrected at voxel level; p < 0.05 FDR-corrected at cluster size), for each session/condition. At this point we look at negative connectivity at whole-brain level, therefore not biasing the analysis toward a specific topology/topography. Then, we investigate the modulation of negative connectivity in these clusters, extracting significant connectivity values for each participant (p < 0.001 uncorrected at voxel level; p < 0.05 FDR-corrected at cluster size; r > 3) at each time point (acute, cumulative, and after tDCS). Values greater/smaller than 2 standard deviations from the mean were removed from the dataset. Finally, a repeated measure analyses of variance (rp-ANOVA) was carried out including the factor "Condition" (active, sham), "Time" (baseline, acute, cumulative, after), and the interaction "Condition × Time." Moreover, as an exploratory analysis we also compared FC values extracted for each time point with the FC value obtained at baseline separately for real and sham net-tDCS by means of paired t-tests

($p < 0.05$) using Statistical Package for Social Science (IBM SPSS Statistics 20) for Windows.

2.11 | Subjective sensations

Given the different spatial distribution of the induced electrical currents (due to the different number, location, and size of the electrodes across montages, with an overall higher total stimulation intensity for multifocal stimulation equal to 4 mA, compared to bifocal stimulation inducing 2 mA), we used a self-report questionnaire (Fertonani et al., 2010) to collect information about subjective sensations during both standard bifocal and network-targeted stimulation, addressing commonly reported subjective feelings (e.g., tingling, pain, headache, etc..) that might be relevant for participant and operator blinding in future studies. We performed a rp-ANOVA testing the factor "Condition" (real and sham), "Montage" (standard bifocal and network targeted), and the interaction "Condition × Montage" for each item of the questionnaire. Moreover, post hoc analyses of simple main effects were performed using pairwise comparisons ($p < 0.05$) in SPSS 20.

3 | RESULTS

3.1 | Connectivity changes in the SMN

The overall ANOVA model was significant ($F_{(2,158)} = 4.25$, $p < 0.003$), with a significant effect of *Montage* ($F_{(2,158)} = 3.58$, $p < 0.007$), as well as an effect of *Condition* ($F_{(2,158)} = 2.62$, $p < 0.012$) and *Time* ($F_{(2,158)} = 3.71$, $p < 0.002$). A significant Montage × Condition × Time interaction was found ($F_{(2,158)} = 2.36$, $p < 0.025$), therefore post hoc comparisons of interest were run to understand the specific acute, cumulative, and after effects of net-tDCS. Similar to that observed using corticospinal excitability in our previous study by Fischer et al. (2017), a significant increase in intrinsic FC of the sensorimotor ICA component (i.e., increased positive connectivity in both motor cortices) was observed both during (ACUTE: $t_{(158)} = 9.86$, $p < 0.03$; CUMULATIVE: $t_{(158)} = 25.81$, $p < 0.006$; Figure 2a,b) and immediately after real net-tDCS (AFTER: $t_{(158)} = 36.14$, $p < 0.002$, Figure 2c), compared to standard tDCS. MNI coordinates of each significant cluster are reported in Table S1.

3.2 | Effect on network-to-network connectivity

A significant effect of *Condition* ($F_{(1,9)} = 5.24$; $p = 0.048$) was observed, whereas no significant results was found for *Time* ($F_{(3,27)} = 1.70$; $p = 0.19$) and for *Condition* × *Time* interaction ($F_{(3,27)} = 1.16$; $p = 0.34$). In order to investigate these results in detail, we conducted several paired *t*-tests ($p < 0.05$) evaluating the differences in all time points (acute, cumulative, and after) between the two conditions (active and sham). The results showed a significant increase of the negative connectivity between SMN and ACC/precuneus for real net-tDCS in all time points when compared to acute sham tDCS (Acute: $t_{(9)} = 2.11$, $p = 0.032$; Cumulative: $t_{(9)} = 2.93$, $p = 0.008$; After: $t_{(9)} = 1.93$, $p = 0.043$; see Figure 3). All remaining contrasts reported no significant results (all $p > 0.08$).

Moreover, the exploratory analysis conducted separately for real and sham net-tDCS comparing FC values extracted for each time point showed an increase of negative connectivity both during (ACUTE and CUMULATIVE) and after stimulation only for real

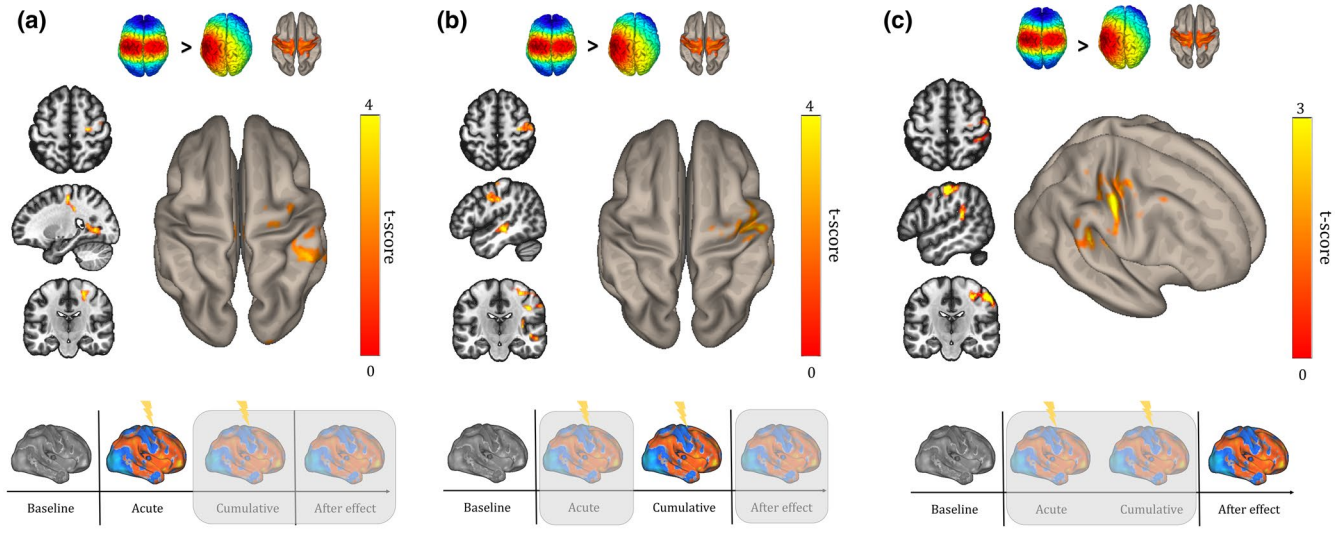

FIGURE 2 Functional connectivity results. Results of the contrasts between standard and net-tDCS for the sensorimotor ICA component are shown for each time point relative to baseline: Acute (a; minute 1–8); Cumulative (b; minute 15–22), and After (c) tDCS effect. The images, displayed in neurological convention, show an increase of functional connectivity in the left hemisphere regioins of the SMN during and after net-tDCS compared to standard tDCS group and with respect to baseline connectivity. Axial, coronal, and sagittal views are shown. MNI coordinates of each significant cluster are reported in Table S1 [Color figure can be viewed at wileyonlinelibrary.com]

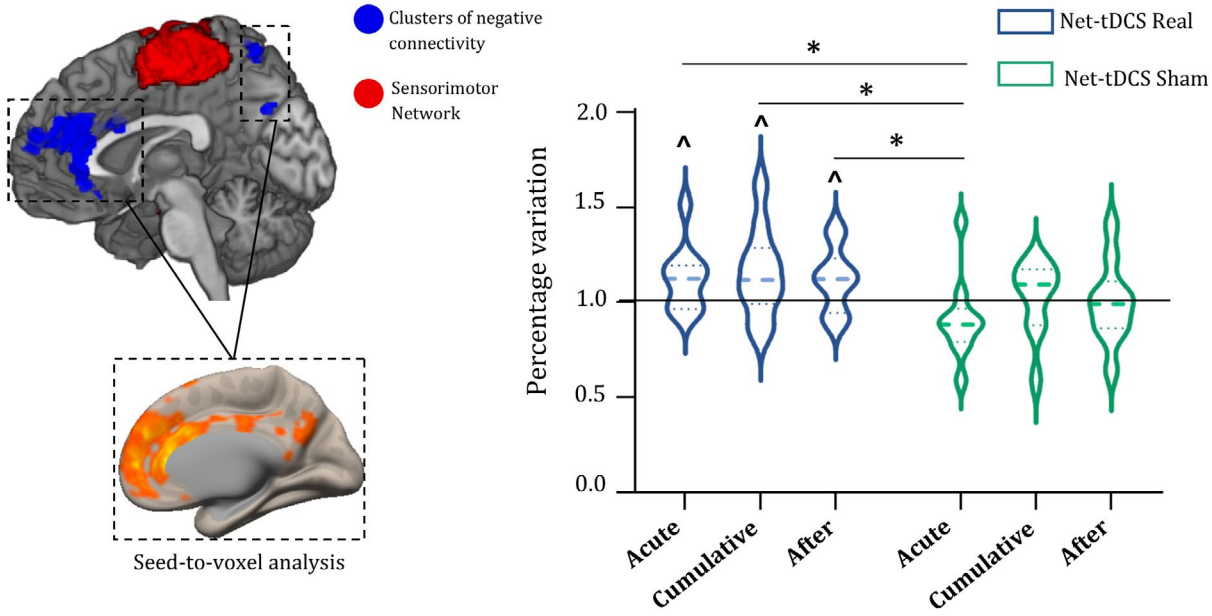

FIGURE 3 Modulation of network-to-network connectivity. Acute, cumulative, and after effect of stimulation on the negative FC is shown for net-tDCS. The plot represents the change in FC as compared to baseline (1 = 100% baseline) at each time point (Acute, Cumulative, and After tDCS; for example, 1.1 equals to 10% increase in FC compared to baseline), for both real and sham net-tDCS. Negatively correlated regions targeted by cathodal stimulation (ACC and Precuneus) are shown. * identifies time points in which the modulation of negative FC is significantly different between conditions ($p < 0.05$), whereas ^ shows the significant effect of real net-tDCS in different time points compared to baseline. [Color figure can be viewed at wileyonlinelibrary.com]

tDCS (ACUTE: $t_{(9)} = -2.28$, $p = 0.024$; CUMULATIVE: $t_{(9)} = -2.09$, $p = 0.033$; AFTER: $t_{(9)} = -2.20$, $p = 0.027$, respectively; % increase in FC for real net-tDCS with respect to baseline: ACUTE: 12%; CUMULATIVE: 15%; AFTER: 11%, respectively). Conversely, the connectivity between SMN and its negatively correlated clusters was not significantly different during or after sham net-tDCS (ACUTE: $t_{(9)} = 1.29$, $p = 0.11$; CUMULATIVE: $t_{(9)} = -0.45$, $p = 0.33$; AFTER: $t_{(9)} = 0.014$, $p = 0.49$, respectively; % increase in FC for sham net-tDCS with respect to baseline: ACUTE: −0.8%; CUMULATIVE: 2%; AFTER: −0.1%, respectively; Figure 3).

3.3 | Induced subjective sensations

Neither side effects nor adverse effects were reported during or after stimulation, confirming the safety profile of both standard and net-tDCS. The reported subjective sensations were not significantly different between stimulation modalities, as showed by the ANOVAs results. In particular, no significant effect was observed for headache (*Montage*: $F_{(1,9)} = 1.80$; $p = 0.21$; *Condition*: $F_{(1,9)} = 0.31$; $p = 0.59$; *Montage* × *Condition*: $F_{(1,9)} = 3.85$; $p = 0.08$); scalp pain (*Montage*: $F_{(1,9)} = 1.55$; $p = 0.24$; *Condition*: $F_{(1,9)} = 0.10$; $p = 0.76$; *Montage* × *Condition*: $F_{(1,9)} = 3.46$; $p = 0.09$); scalp burn (*Montage*: $F_{(1,9)} = 0.10$; $p = 0.76$; *Condition*: $F_{(1,9)} = 0.00$; $p = 1$; *Montage* × *Condition*: $F_{(1,9)} = 0.23$; $p = 0.64$); sensation under the electrodes (*Montage*: $F_{(1,9)} = 0.03$; $p = 0.86$; *Condition*: $F_{(1,9)} = 0.80$; $p = 0.39$; *Montage* × *Condition*: $F_{(1,9)} = 3.12$; $p = 0.11$); sleepiness (*Montage*: $F_{(1,9)} = 2.71$; $p = 0.13$; *Condition*: $F_{(1,9)} = 0.37$; $p = 0.56$; *Montage* × *Condition*: $F_{(1,9)} = 0.37$; $p = 0.56$); trouble in concentrating (*Montage*: $F_{(1,9)} = 2.44$; $p = 0.15$; *Condition*: $F_{(1,9)} = 2.25$; $p = 0.17$; *Montage* × *Condition*: $F_{(1,9)} = 0.00$; $p = 1$); and change in mood (*Montage*: $F_{(1,9)} = 0.79$; $p = 0.40$; *Condition*: $F_{(1,9)} = 0.31$; $p = 0.59$; *Montage* × *Condition*: $F_{(1,9)} = 3.86$; $p = 0.3$). A significant effect of *Montage* ($F_{(1,9)} = 7.36$; $p = 0.02$) was observed for the item "skin redness," whereas no significant effects of Condition ($F_{(1,9)} = 2.25$; $p = 0.17$) and Condition × Montage ($F_{(1,9)} = 2.25$; $p = 0.17$) were observed. Post hoc analysis conducted on this item confirmed the higher skin redness after real standard stimulation ($t_{(9)} = 2.23$; $p = 0.038$) compared to the real net-tDCS. For the real tDCS conditions, higher scores were observed for (i) sleepiness (mostly imputed to the length of the study visits), (ii) tingling under the electrodes (usually reported at the beginning of stimulation and decreasing afterwards), and (iii) burning (mild, not reported as uncomfortable), but none of these aspects resulted significant different compared to the sham conditions. Most commonly reported effects were headache, changes in mood, neck pain, scalp pain, and trouble concentrating. Individual scores are reported in Figure 4, mean and standard deviation (*SD*) for each item by condition and montage are shown in Table S2.

4 | DISCUSSION

The aim of the study was to further explore previous findings reported by Fischer et al. (2017) using TMS-EMG (i.e., net-tDCS is able to modulate the entire SMN beyond the effect of canonical bifocal

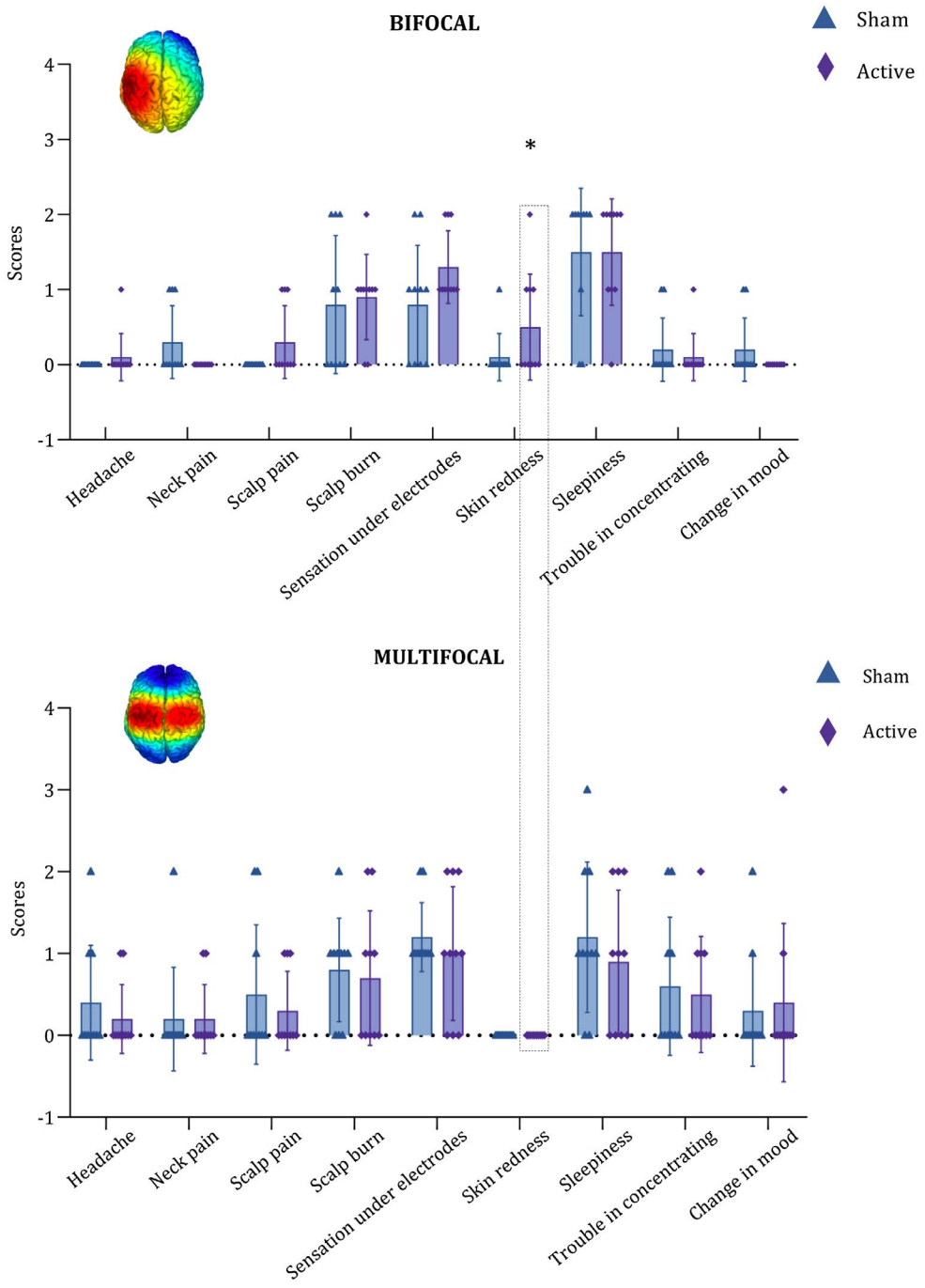

FIGURE 4 Side effects. Bars represent average subjective reports (Lickert scale: 0 = none, 4 = strong, adapted from Fertonani et al., 2010) for both standard bifocal and net-tDCS. Blue triangles and violet diamond represent the subjects' single value reported respectively for sham and real conditions. Error bars represent standard error of mean. $^{*}p < 0.05$ [Color figure can be viewed at wileyonlinelibrary.com]

tDCS over left M1), by using a concurrent tDCS-fMRI approach while also investigating the feasibility, efficacy, and safety of a tDCS solution optimized to engage a target RSN via multichannel stimulation. Moreover, the present study was designed to test the possibility of using net-tDCS to modulate not only local brain dynamics but also the interplay between the target networks and its negatively correlated brain regions/networks. As predicted, results suggest a stronger engagement of the bilateral sensorimotor areas during net-tDCS compared to bifocal tDCS. Furthermore, preliminary results also support its efficacy in amplifying the negative connectivity between the SMN and its negatively correlated brain regions targeted by cathodal stimulation. However, due to the small sample size, this result should be interpreted carefully and requires further validation. Findings might be relevant for the optimization of tDCS in clinical contexts, where alteration of network-to-network connectivity have been documented (e.g., see Zhou et al., 2010), as well as for cognitive enhancement purposes (Santarnecchi et al., 2017; Spreng, Stevens, Viviano, & Schacter, 2016).

4.1 | Modulation of intrinsic FC

Modulation of M1 excitability via tDCS has been extensively used to enhance motor behavior and motor learning (Nitsche et al., 2003; Reis et al., 2009), also exploring its potential in clinical and rehabilitative settings (Liew et al., 2014). Several studies have also investigated the impact of tDCS by combining TMS-EEG (Pellicciari et al., 2013; Romero Lauro et al., 2014; Varoli et al., 2018) or by means of neuroimaging measures (Amadi, Ilie, Johansen-Berg, & Stagg, 2014; Polanía, Paulus, & Nitsche, 2012a, 2012b; Sehm, Kipping, Schäfer, Villringer, & Ragert, 2013). Given the shift in focus toward network-based approaches for the study of human cognition (Pisoni et al., 2018; Santarnecchi et al., 2017; Santarnecchi, Momi, et al., 2018; Santarnecchi, Sprugnoli, et al., 2018; Spreng et al., 2016) —and more recently even for the diagnosis of neuropsychiatric conditions (Fox et al., 2014)— we tested the impact of a tDCS montage optimized to concurrently modulate multiple nodes of the SMN (and its negatively correlated regions) instead of just left M1. Using a multifocal tDCS solution previously tested by our group (Fischer et al., 2017), here we document a greater modulation of FC involving both left and right M1 during net-tDCS compared to standard tDCS, similar to that observed in our previous study where an increase in excitability of right M1 was found solely for net-tDCS. Moreover, the effect on fMRI connectivity seemed present both during and after tDCS, similar to that we observed in our previous investigation and to that has been reported for standard and high-density (HD) tDCS (Antal et al., 2011; Bikson, Datta, Rahman, & Scaturro, 2010; Dmochowski, Datta, Bikson, Su, & Parra, 2011; Nitsche & Paulus, 2001). This suggests an interesting convergence between neurophysiological findings (i.e., motor-evoked potentials as measured via combined TMS and electromyography) and neuroimaging results related to net-tDCS.

Of note, changes in cortical excitability in one hemisphere could increase or decrease cortical excitability in the other hemisphere by means of interhemispheric connections, such that functional inhibition or excitation of contralateral homologous areas may occur at different times depending on the task at hand/brain state (Bloom & Hynd, 2005). When dealing specifically with the primary motor cortices, neurophysiological and neuroimaging research investigating interhemispheric interactions have corroborated the idea of these two areas being negatively correlated when subjects perform a unimanual motor task (Ferbert et al., 1992; Kobayashi, Hutchinson, Schlaug, & Pascual-Leone, 2003; Vines, Nair, & Schlaug, 2006). The network-targeted solution investigated in the present study offers interesting opportunities to target a bilaterally distributed network, but it should be considered that this might only apply to a healthy brain stimulated at rest. Ad-hoc investigations are needed to adapt net-tDCS for applications in clinical populations with pathological interhemispheric imbalance (such as stroke patients) or those with unilateral lesions in general, for which a reduction of interhemispheric connections has been reported in favor of greater intrahemispheric cohesion (Siegel et al., 2016).

4.2 | Effect on network-to-network connectivity

A growing body of literature suggests the importance of looking at alteration of brain networks, as well as network-to-network interactions, as potential biomarkers of neurological and psychiatric conditions. For instance, alteration of the interplay between the default mode network (DMN) and anterior salience network (ASN) have been documented in both Alzheimer's disease and frontotemporal dementia patients; however, while the former shows increased DMN-AS FC, the latter display the opposite pattern, even though both conditions share a significant neuropathological substrate. This highlights the need for network-targeted interventions able to modulate such dysfunctional inter-network dynamics. Moreover, the negative connectivity (or "anticorrelation") between brain networks has been also promoted as a crucial aspect of the functional organization of the human brain, with relevance for cognitive performance (Fox et al., 2005). For instance, recent reports have highlighted how the strength of the negative connectivity between regions of the dorsal attention network (DAN) and the DMN is among the best predictors of individual variability in intelligence levels (Santarnecchi et al., 2017). Recent work by our group has shown the possibility to selectively modify resting-state fMRI network-to-network coupling by means of multisite TMS using cortico-cortical paired associative stimulation (cc-PAS; Santarnecchi, Momi, et al., 2018); however, the possibility to modulate inter-network dynamics by means of network-targeted tDCS has not been demonstrated yet. Here we show how a tDCS montage optimized to desynchronize the target network (SMN) and its negatively correlated nodes is partially able to increase the negative connectivity between networks. By systematically placing cathodal electrodes over frontal and parietal brain regions (i.e., Fz to target the medial prefrontal cortex and ACC; P3/P4 to target the left/right angular gyrus), net-tDCS resulted in an amplified negative correlation between SMN, ACC, and bilateral angular gyri, compared to the results obtained in the acute sham net-tDCS, but not in the other time points. Even though the presented results are not corrected for FDR at voxel level, they originally suggest the opportunity of manipulating network-to-network FC patterns by means of optimized tDCS targeting both positively and negatively connected brain regions. Moreover, looking at active or sham stimulation alone, a significant trend in the increase of negative connectivity both during and after real net-tDCS compared to baseline was found, with no effect during sham stimulation. While this is suggestive of potential modulation of network-to-network connectivity, this finding should be interpreted carefully given the very limited sample size and high number of conditions/comparisons in the design.

4.3 | Limitations and future directions

The first limitation is represented by the small sample size, which has had a significant impact on data analysis and our ability to draw firm conclusions about some findings, especially those related to modulation of negative connectivity. For these reasons, our study only

represents a preliminary yet informative investigation on the potential of network-targeted tDCS for modulation of network dynamics as compared to bifocal tDCS. Another potential limitation is the higher total current intensity induced by net-tDCS (4 mA) compared to bifocal stimulation (2 mA). In fact, given the nature of multichannel stimulation and the need to target multiple brain regions, net-tDCS is usually performed at higher stimulation intensity compared to standard tDCS, although in a distributed manner through the use of multiple electrodes (eight in this study). Although the flexibility of multichannel systems is an advantage, it comes with the challenge of fine-tuning electrode locations and the currents delivered at each electrode, with increasing demands on the number of electrodes and total current injected if the cortical areas to stimulate are large. Presently, Stimweaver is used with a limitation on maximal electrode current and the total injected current by the montage at any given time. However, this is a conservative criterion, since the potential damage to brain tissues is related to local current and electric field (ohmic power dissipation) in brain tissues, which is not directly related to individual or total electrode current – it depends on the montage specifics. Future work may consider relaxing the condition of total injected current and instead analyze the electric field distribution in the cortex for safety, which will facilitate the design of montages to large widespread cortical networks using many electrodes. Another physical limitation in tES is that because of the governing equations, it is not possible to uniformly stimulate a large cortical patch with, e.g., excitatory fields: the interplay between current flow and anatomy of gyri and sulci makes the presence of electric field orientation stripes unavoidable (Lafon, Rahman, Bikson, & Parra 2017). The use of denser montages can also mitigate this problem.

In addition, TMS-based MEPs should be collected before and after the fMRI-tDCS sessions to provide a comparison between electrophysiological and fMRI effects, also replicating findings from Fischer et al. (2017) and further looking for the predictive power of baseline cortical excitability over tDCS modulation of FC. Moreover, an additional limitation of rs-fMRI technique should be considered. Functional RSNs have been mostly studied through fMRI, with several investigations focused on fMRI-based connectivity dynamics within and across distributed brain networks. However, rs-fMRI is a low temporal resolution estimate of FC, unable to capture brain oscillatory rhythms reflective of actual neural activity (i.e., at millisecond timescale; He, Zempel, Snyder, & Raichle, 2010). Only direct external manipulation of RSN activity may provide valuable information about fast-evolving interactions between RSNs. An increasing number of studies over the years have employed multimodal neuroimaging techniques to better understand the neural origins and spatial – temporal signatures of RSNs (Britz, Van De Ville, & Michel, 2010; Chang, Liu, Chen, Liu, & Duyn, 2013; Chen, Feng, Zhao, Yin, & Wang, 2008; Feige et al., 2017; Laufs, 2008; Liu, Ganzetti, Wenderoth, & Mantini, 2018; Sadaghiani et al., 2010; Tagliazucchi, von Wegner, Morzelewski, Brodbeck, & Laufs, 2012). For example, some studies examined the specificity of tDCS effects on brain connectivity by means of TMS-EEG, highlighting how the spread of tDCS effects follows structural brain connections when applied at rest (Romero Lauro et al., 2014), whereas spreading only to functionally relevant areas when tDCS is applied during task execution (Pisoni et al., 2018). Moreover, recent work by our group (Ozdemir et al., 2020) has revealed that is it possible to capture the same fMRI dynamics but with high temporal resolution by using network-guided TMS-EEG. Despite the fact that no consensus has been reached on the correlation between EEG spectral power features and dynamic FC profiles within or across specific RSNs, multifocal tDCS approaches could be helpful in investigating this link.

Future studies should also investigate other control conditions (e.g., inverse condition, extracephalic cathodal electrode) and the possibility of personalizing electrode montages (i.e., electrode number and intensity) based on individual brain anatomy (Tecchio et al., 2013, Ruffini et al., 2018) and fMRI network dynamics/topology, like recently shown in a similar network-target brain stimulation approach using personalized multi-coil TMS (Santarnecchi, Momi, et al., 2018).

5 | CONCLUSION

Multifocal tDCS solutions informed by resting-state fMRI connectivity patterns and realistic head models can increase the precision of brain networks targeting in humans, with the possibility of inducing effects on multiple network nodes at the same time while affecting both local and network-to-network connectivity dynamics.

DECLARATION OF TRANSPARENCY

The authors, reviewers and editors affirm that in accordance to the policies set by the *Journal of Neuroscience Research*, this manuscript presents an accurate and transparent account of the study being reported and that all critical details describing the methods and results are present.

ACKNOWLEDGMENTS

The authors thank all the participants who took part in the study and for their efforts. Dr. Pascual-Leone and Dr. Santarnecchi are partially supported by Office of the Director of National Intelligence (ODNI), Intelligence Advanced Research Projects Activity (IARPA), via 2014- 13121700007. The views and conclusions contained herein are those of the authors and should not be interpreted as necessarily representing the official policies or endorsements, either expressed or implied, of the ODNI, IARPA, or the U.S. Government. Pascual-Leone is further supported by the Berenson-Allen Foundation, the Sidney R. Baer Jr. Foundation, grants from the National Institutes of Health (R01HD069776, R01NS073601, R21 MH099196, R21 NS082870, R21 NS085491, R21 HD07616), and Harvard Catalyst | The Harvard Clinical and Translational Science Center (NCRR and the NCATS NIH, UL1 RR025758). Dr. Santarnecchi is supported by the Beth Israel Deaconess Medical Center (BIDMC) via the Chief Academic Officer (CAO) Award 2017, the Defence Advanced Research Projects Agency (DARPA) via HR001117S0030, and the NIH (P01 AG031720-06A1, R01

MH117063-01, R01 AG060981-01). Dr. Giulio Ruffini is partially supported by the European FET Open project Luminous (European Union's Horizon 2020 research and innovation programme under grant agreement no. 686764). The content of this paper is solely the responsibility of the authors and does not necessarily represent the official views of Harvard University, its affiliated academic healthcare centers and the National Institutes of Health.

CONFLICT OF INTEREST

Giulio Ruffini is a shareholder and works for Neuroelectrics, a company developing medical devices for NIBS. Ricardo Salvador works for Neuroelectrics.

AUTHOR CONTRIBUTIONS

Conceptualization, E.S. and G.R.; *Methodology*, E.S., G.R., and R.S.; *Investigation*, L.Me., L.Mo., and F.N.; *Software*, E.S., G.R., and R.S.; *Formal Analysis*, L.Me, A.M., D.M., and E.S.; *Writing – Original Draft*, L.Me.; *Writing – Review & Editing*, G.S., A.M., S.R.,G.R. and E.S.; *Resources*, G.R. and E.S.; *Supervision*, A.P.-L., A.R., S.R., and E.S.

PEER REVIEW

The peer review history for this article is available at https://publons.com/publon/10.1002/jnr.24690.

DATA AVAILABILITY STATEMENT

The data that support the findings of this study are available from the corresponding author upon reasonable request.

ORCID

Emiliano Santarnecchi https://orcid.org/0000-0002-6533-7427

REFERENCES

Amadi, U., Ilie, A., Johansen-Berg, H., & Stagg, C. J. (2014). Polarity-specific effects of motor transcranial direct current stimulation on fMRI resting state networks. *NeuroImage*, *88*, 155–161. https://doi.org/10.1016/j.neuroimage.2013.11.037

Antal, A., Polania, R., Schmidt-Samoa, C., Dechent, P., & Paulus, W. (2011). Transcranial direct current stimulation over the primary motor cortex during fMRI. *NeuroImage*, *55*(2), 590–596. https://doi.org/10.1016/j.neuroimage.2010.11.085

Antal, A., Terney, D., Poreisz, C., & Paulus, W. (2007). Towards unravelling task-related modulations of neuroplastic changes induced in the human motor cortex. *European Journal of Neuroscience*, *26*(9), 2687–2691. https://doi.org/10.1111/j.1460-9568.2007.05896.x

Beckmann, C. F., & Smith, S. M. (2005). Tensorial extensions of independent component analysis for multisubject FMRI analysis. *NeuroImage*, *25*(1), 294–311. https://doi.org/10.1016/j.neuroimage.2004.10.043

Bikson, M., Datta, A., Rahman, A., & Scaturro, J. (2010). Electrode montages for tDCS and weak transcranial electrical stimulation: Role of "return" electrode's position and size. *Clinical Neurophysiology*, *121*(12), 1976–1978. https://doi.org/10.1016/j.clinph.2010.05.020

Bloom, J. S., & Hynd, G. W. (2005). The role of the corpus callosum in interhemispheric transfer of information: Excitation or inhibition? *Neuropsychology Review*, *15*(2), 59–71. https://doi.org/10.1007/s11065-005-6252-y

Boros, K., Poreisz, C., Münchau, A., Paulus, W., & Nitsche, M. A. (2008). Premotor transcranial direct current stimulation (tDCS) affects primary motor excitability in humans. *European Journal of Neuroscience*, *27*(5), 1292–1300. https://doi.org/10.1111/j.1460-9568.2008.06090.x

Britz, J., Van De Ville, D., & Michel, C. M. (2010). BOLD correlates of EEG topography reveal rapid resting-state network dynamics. *NeuroImage*, *52*(4), 1162–1170. https://doi.org/10.1016/j.neuroimage.2010.02.052

Chang, C., Liu, Z., Chen, M. C., Liu, X., & Duyn, J. H. (2013). EEG correlates of time-varying BOLD functional connectivity. *NeuroImage*, *72*, 227–236. https://doi.org/10.1016/j.neuroimage.2013.01.049

Chen, A. C. N., Feng, W., Zhao, H., Yin, Y., & Wang, P. (2008). EEG default mode network in the human brain: Spectral regional field powers. *NeuroImage*, *41*(2), 561–574. https://doi.org/10.1016/j.neuroimage.2007.12.064

Corbetta, M. (1998). Frontoparietal cortical networks for directing attention and the eye to visual locations: Identical, independent, or overlapping neural systems? *Proceedings of the National Academy of Sciences of the United States of America*, *95*(3), 831–838. https://doi.org/10.1073/pnas.95.3.831

Dmochowski, J. P., Datta, A., Bikson, M., Su, Y., & Parra, L. C. (2011). Optimized multi-electrode stimulation increases focality and intensity at target. *Journal of Neural Engineering*, *8*(4), 046011. https://doi.org/10.1088/1741-2560/8/4/046011

Drysdale, A. T., Grosenick, L., Downar, J., Dunlop, K., Mansouri, F., Meng, Y., … Liston, C. (2017). Resting-state connectivity biomarkers define neurophysiological subtypes of depression. *Nature Medicine*, *23*(1), 28–38. https://doi.org/10.1038/nm.4246

Feige, B., Spiegelhalder, K., Kiemen, A., Bosch, O. G., Tebartz van Elst, L., Hennig, J., … Riemann, D. (2017). Distinctive time-lagged resting-state networks revealed by simultaneous EEG-fMRI. *NeuroImage*, *145*, 1–10. https://doi.org/10.1016/j.neuroimage.2016.09.027

Ferbert, A., Priori, A., Rothwell, J. C., Day, B. L., Colebatch, J. G., & Marsden, C. D. (1992). Interhemispheric inhibition of the human motor cortex. *Journal of Physiology*, *453*(1), 525–546. https://doi.org/10.1113/jphysiol.1992.sp019243

Fertonani, A., Rosini, S., Cotelli, M., Rossini, P. M., & Miniussi, C. (2010). Naming facilitation induced by transcranial direct current stimulation. *Behavioural Brain Research*, *208*(2), 311–318. https://doi.org/10.1016/j.bbr.2009.10.030

Fischer, D. B., Fried, P. J., Ruffini, G., Ripolles, O., Salvador, R., Banus, J., … Fox, M. D. (2017). Multifocal tDCS targeting the resting state motor network increases cortical excitability beyond traditional tDCS targeting unilateral motor cortex. *NeuroImage*, *157*, 34–44. https://doi.org/10.1016/j.neuroimage.2017.05.060

Fox, M. D. (2018). Mapping symptoms to brain networks with the human connectome. *New England Journal of Medicine*, *379*(23), 2237–2245. https://doi.org/10.1056/NEJMra1706158

Fox, M. D., Buckner, R. L., Liu, H., Chakravarty, M. M., Lozano, A. M., & Pascual-Leone, A. (2014). Resting-state networks link invasive and noninvasive brain stimulation across diverse psychiatric and neurological diseases. *Proceedings of the National Academy of Sciences of the United States of America*, *111*(41), E4367–E4375. https://doi.org/10.1073/pnas.1405003111

Fox, M. D., Buckner, R. L., White, M. P., Greicius, M. D., & Pascual-Leone, A. (2012). Efficacy of transcranial magnetic stimulation targets for depression is related to intrinsic functional connectivity with the subgenual cingulate. *Biological Psychiatry*, *72*(7), 595–603. https://doi.org/10.1016/j.biopsych.2012.04.028

Fox, M. D., Snyder, A. Z., Vincent, J. L., Corbetta, M., Essen, D. C. V., & Raichle, M. E. (2005). The human brain is intrinsically organized into dynamic, anticorrelated functional networks. *Proceedings of the National Academy of Sciences of the United States of America*, *102*(27), 9673–9678. https://doi.org/10.1073/pnas.0504136102

Fritsch, B., Reis, J., Martinowich, K., Schambra, H. M., Ji, Y., Cohen, L. G., & Lu, B. (2010). Direct current stimulation promotes BDNF-dependent synaptic plasticity: Potential implications for motor

learning. *Neuron*, *66*(2), 198–204. https://doi.org/10.1016/j.neuron.2010.03.035

Furubayashi, T., Terao, Y., Arai, N., Okabe, S., Mochizuki, H., Hanajima, R., … Ugawa, Y. (2008). Short and long duration transcranial direct current stimulation (tDCS) over the human hand motor area. *Experimental Brain Research*, *185*(2), 279–286. https://doi.org/10.1007/s00221-007-1149-z

He, B. J., Zempel, J. M., Snyder, A. Z., & Raichle, M. E. (2010). The temporal structures and functional significance of scale-free brain activity. *Neuron*, *66*(3), 353–369. https://doi.org/10.1016/j.neuron.2010.04.020

Kobayashi, M., Hutchinson, S., Schlaug, G., & Pascual-Leone, A. (2003). Ipsilateral motor cortex activation on functional magnetic resonance imaging during unilateral hand movements is related to interhemispheric interactions. *NeuroImage*, *20*(4), 2259–2270. https://doi.org/10.1016/S1053-8119(03)00220-9

Lafon, B., Rahman, A., Bikson, M., & Parra, L. C. (2017). Direct current stimulation alters neuronal input/output function. *Brain Stimulation*, *10*(1), 36–45. https://doi.org/10.1016/j.brs.2016.08.014

Laufs, H. (2008). Endogenous brain oscillations and related networks detected by surface EEG-combined fMRI. *Human Brain Mapping*, *29*(7), 762–769. https://doi.org/10.1002/hbm.20600

Lefaucheur, J.-P., Antal, A., Ayache, S. S., Benninger, D. H., Brunelin, J., Cogiamanian, F., … Paulus, W. (2017). Evidence-based guidelines on the therapeutic use of transcranial direct current stimulation (tDCS). *Clinical Neurophysiology*, *128*(1), 56–92. https://doi.org/10.1016/j.clinph.2016.10.087

Liew, S. L., Santarnecchi, E., Buch, E. R., & Cohen, L. G. (2014). Non-invasive brain stimulation in neurorehabilitation: Local and distant effects for motor recovery. *Frontiers in Human Neuroscience*, *8*, 1662–5161. https://doi.org/10.3389/fnhum.2014.00378

Lindenberg, R., Nachtigall, L., Meinzer, M., Sieg, M. M., & Floel, A. (2013). Differential effects of dual and unihemispheric motor cortex stimulation in older adults. *Journal of Neuroscience*, *33*(21), 9176–9183. https://doi.org/10.1523/JNEUROSCI.0055-13.2013

Liu, Q., Ganzetti, M., Wenderoth, N., & Mantini, D. (2018). Detecting large-scale brain networks using EEG: Impact of electrode density, head modeling and source localization. *Frontiers in Neuroinformatics*, *12*, 4. https://doi.org/10.3389/fninf.2018.00004

Meinzer, M., Antonenko, D., Lindenberg, R., Hetzer, S., Ulm, L., Avirame, K., … Flöel, A. (2012). Electrical brain stimulation improves cognitive performance by modulating functional connectivity and task-specific activation. *Journal of Neuroscience*, *32*(5), 1859–1866. https://doi.org/10.1523/JNEUROSCI.4812-11.2012

Meinzer, M., Lindenberg, R., Antonenko, D., Flaisch, T., & Flöel, A. (2013). Anodal transcranial direct current stimulation temporarily reverses age-associated cognitive decline and functional brain activity changes. *Journal of Neuroscience*, *33*(30), 12470–12478. https://doi.org/10.1523/JNEUROSCI.5743-12.2013

Miranda, P. C., Mekonnen, A., Salvador, R., & Ruffini, G. (2013). The electric field in the cortex during transcranial current stimulation. *NeuroImage*, *70*, 48–58. https://doi.org/10.1016/j.neuroimage.2012.12.034

Nitsche, M. A., & Paulus, W. (2000). Excitability changes induced in the human motor cortex by weak transcranial direct current stimulation. *Journal of Physiology*, *527*(3), 633–639. https://doi.org/10.1111/j.1469-7793.2000.t01-1-00633.x

Nitsche, M. A., & Paulus, W. (2001). Sustained excitability elevations induced by transcranial DC motor cortex stimulation in humans. *Neurology*, *57*(10), 1899–1901. https://doi.org/10.1212/WNL.57.10.1899

Nitsche, M. A., Schauenburg, A., Lang, N., Liebetanz, D., Exner, C., Paulus, W., & Tergau, F. (2003). Facilitation of implicit motor learning by weak transcranial direct current stimulation of the primary motor cortex in the human. *Journal of Cognitive Neuroscience*, *15*(4), 619–626. https://doi.org/10.1162/089892903321662994

Nitsche, M. A., Seeber, A., Frommann, K., Klein, C. C., Rochford, C., Nitsche, M. S., … Tergau, F. (2005). Modulating parameters of excitability during and after transcranial direct current stimulation of the human motor cortex. *Journal of Physiology*, *568*(1), 291–303. https://doi.org/10.1113/jphysiol.2005.092429

Ozdemir, R. A., Tadayon, E., Boucher, P., Momi, D., Karakhanyan, K. A., Fox, M. D., … Santarnecchi, E. (2020). Individualized perturbation of the human connectome reveals reproducible biomarkers of network dynamics relevant to cognition. *Proceedings of the National Academy of Sciences of the United States of America*, *117*(14), 8115–8125. https://doi.org/10.1073/pnas.1911240117

Paulus, W. (2003). Chapter 26 Transcranial direct current stimulation (tDCS). In W. Paulus, F. Tergau, M. A. Nitsche, J. G. Rothwell, U. Ziemann, & M. Hallett (Eds.), *Supplements to clinical neurophysiology* (Vol. *56*, pp. 249–254). Gottingen, Germany: Elsevier. https://doi.org/10.1016/S1567-424X(09)70229-6

Pellicciari, M. C., Brignani, D., & Miniussi, C. (2013). Excitability modulation of the motor system induced by transcranial direct current stimulation: A multimodal approach. *NeuroImage*, *83*, 569–580. https://doi.org/10.1016/j.neuroimage.2013.06.076

Pisoni, A., Mattavelli, G., Papagno, C., Rosanova, M., Casali, A. G., & Romero Lauro, L. J. (2018). Cognitive enhancement induced by anodal tDCS drives circuit-specific cortical plasticity. *Cerebral Cortex*, *28*(4), 1132–1140. https://doi.org/10.1093/cercor/bhx021

Polanía, R., Nitsche, M. A., & Paulus, W. (2011). Modulating functional connectivity patterns and topological functional organization of the human brain with transcranial direct current stimulation. *Human Brain Mapping*, *32*(8), 1236–1249. https://doi.org/10.1002/hbm.21104

Polanía, R., Paulus, W., & Nitsche, M. A. (2012a). Modulating cortico-striatal and thalamo-cortical functional connectivity with transcranial direct current stimulation. *Human Brain Mapping*, *33*(10), 2499–2508. https://doi.org/10.1002/hbm.21380

Polanía, R., Paulus, W., & Nitsche, M. A. (2012b). Reorganizing the intrinsic functional architecture of the human primary motor cortex during rest with non-invasive cortical stimulation. *PLoS One*, *7*(1), e30971. https://doi.org/10.1371/journal.pone.0030971

Reis, J., Schambra, H. M., Cohen, L. G., Buch, E. R., Fritsch, B., Zarahn, E., … Krakauer, J. W. (2009). Noninvasive cortical stimulation enhances motor skill acquisition over multiple days through an effect on consolidation. *Proceedings of the National Academy of Sciences of the United States of America*, *106*(5), 1590–1595. https://doi.org/10.1073/pnas.0805413106

Romero Lauro, L. J., Rosanova, M., Mattavelli, G., Convento, S., Pisoni, A., Opitz, A., … Vallar, G. (2014). TDCS increases cortical excitability: Direct evidence from TMS–EEG. *Cortex*, *58*, 99–111. https://doi.org/10.1016/j.cortex.2014.05.003

Ruffini, G., Fox, M. D., Ripolles, O., Miranda, P. C., & Pascual-Leone, A. (2014). Optimization of multifocal transcranial current stimulation for weighted cortical pattern targeting from realistic modeling of electric fields. *NeuroImage*, *89*, 216–225. https://doi.org/10.1016/j.neuroimage.2013.12.002

Ruffini, G., Wendling, F., Merlet, I., Molaee-Ardekani, B., Mekonnen, A., Salvador, R., … Miranda, P. C. (2013). Transcranial current brain stimulation (tCS): Models and technologies. *IEEE Transactions on Neural Systems and Rehabilitation Engineering*, *21*(3), 333–345. https://doi.org/10.1109/TNSRE.2012.2200046

Ruffini, Giulio, Wendling, F., Sanchez-Todo, R., & Santarnecchi, E. (2018). Targeting brain networks with multichannel transcranial current stimulation (tCS). *Current Opinion in BioMedical Engineering.8*, 70–77.

Sadaghiani, S., Scheeringa, R., Lehongre, K., Morillon, B., Giraud, A.-L., & Kleinschmidt, A. (2010). Intrinsic connectivity networks, alpha oscillations, and tonic alertness: A simultaneous electroencephalography/functional magnetic resonance imaging study. *Journal of Neuroscience*, *30*(30), 10243–10250. https://doi.org/10.1523/JNEUROSCI.1004-10.2010

Sánchez-Kuhn, A., Pérez-Fernández, C., Cánovas, R., Flores, P., & Sánchez-Santed, F. (2017). Transcranial direct current stimulation as a motor

neurorehabilitation tool: An empirical review. *BioMedical Engineering OnLine*, *16*(1), 76. https://doi.org/10.1186/s12938-017-0361-8

Santarnecchi, E., Emmendorfer, A., Tadayon, S., Rossi, S., Rossi, A., & Pascual-Leone, A. (2017). Network connectivity correlates of variability in fluid intelligence performance. *Intelligence*, *65*, 35–47. https://doi.org/10.1016/j.intell.2017.10.002

Santarnecchi, E., Momi, D., Sprugnoli, G., Neri, F., Pascual-Leone, A., Rossi, A., & Rossi, S. (2018). Modulation of network-to-network connectivity via spike-timing-dependent noninvasive brain stimulation. *Human Brain Mapping*, *39*(12), 4870–4883. https://doi.org/10.1002/hbm.24329

Santarnecchi, E., Sprugnoli, G., Tatti, E., Mencarelli, L., Neri, F., Momi, D., … Rossi, A. (2018). Brain functional connectivity correlates of coping styles. *Cognitive, Affective, & Behavioral Neuroscience*, *18*(3), 495–508. https://doi.org/10.3758/s13415-018-0583-7

Sehm, B., Kipping, J., Schäfer, A., Villringer, A., & Ragert, P. (2013). A comparison between uni- and bilateral tDCS effects on functional connectivity of the human motor cortex. *Frontiers in Human Neuroscience*, *7*(183), 1–7. https://doi.org/10.3389/fnhum.2013.00183

Sheffield, J. M., & Barch, D. M. (2016). Cognition and resting-state functional connectivity in schizophrenia. *Neuroscience & Biobehavioral Reviews*, *61*, 108–120. https://doi.org/10.1016/j.neubiorev.2015.12.007

Siegel, J. S., Ramsey, L. E., Snyder, A. Z., Metcalf, N. V., Chacko, R. V., Weinberger, K., … Corbetta, M. (2016). Disruptions of network connectivity predict impairment in multiple behavioral domains after stroke. *Proceedings of the National Academy of Sciences of the United States of America*, *113*(30), E4367–E4376. https://doi.org/10.1073/pnas.1521083113

Spreng, R. N., Stevens, W. D., Viviano, J. D., & Schacter, D. L. (2016). Attenuated anticorrelation between the default and dorsal attention networks with aging: Evidence from task and rest. *Neurobiology of Aging*, *45*, 149–160. https://doi.org/10.1016/j.neurobiolaging.2016.05.020

Tagliazucchi, E., von Wegner, F., Morzelewski, A., Brodbeck, V., & Laufs, H. (2012). Dynamic BOLD functional connectivity in humans and its electrophysiological correlates. *Frontiers in Human Neuroscience*, *6*(339), 1–22. https://doi.org/10.3389/fnhum.2012.00339

Tecchio, F., Cancelli, A., Cottone, C., Tomasevic, L., Devigus, B., Zito, G., … Carducci, F. (2013). Regional personalized electrodes to select transcranial current stimulation target. *Frontiers in Human Neuroscience*, *7*(131), 1–5. https://doi.org/10.3389/fnhum.2013.00131

Uy, J., Ridding, M. C., Hillier, S., Thompson, P. D., & Miles, T. S. (2003). Does induction of plastic change in motor cortex improve leg function after stroke? *Neurology*, *61*(7), 982–984. https://doi.org/10.1212/01.WNL.0000078809.33581.1F

van Asseldonk, E. H. F., & Boonstra, T. A. (2016). Transcranial direct current stimulation of the leg motor cortex enhances coordinated motor output during walking with a large inter-individual variability. *Brain Stimulation*, *9*(2), 182–190. https://doi.org/10.1016/j.brs.2015.10.001

Varoli, E., Pisoni, A., Mattavelli, G. C., Vergallito, A., Gallucci, A., Mauro, L. D., … Romero Lauro, L. J. (2018). Tracking the effect of cathodal transcranial direct current stimulation on cortical excitability and connectivity by means of TMS-EEG. *Frontiers in Neuroscience*, *12*, 319. https://doi.org/10.3389/fnins.2018.00319

Vines, B. W., Nair, D. G., & Schlaug, G. (2006). Contralateral and ipsilateral motor effects after transcranial direct current stimulation. *NeuroReport*, *17*(6), 671–674. https://doi.org/10.1097/00001756-200604240-00023

Whitfield-Gabrieli, S., & Nieto-Castanon, A. (2012). Conn: A functional connectivity toolbox for correlated and anticorrelated brain networks. *Brain Connect*, *2*(3), 125–141. https://doi.org/10.1089/brain.2012.0073

Zheng, X., Alsop, D. C., & Schlaug, G. (2011). Effects of transcranial direct current stimulation (tDCS) on human regional cerebral blood flow. *NeuroImage*, *58*(1), 26–33. https://doi.org/10.1016/j.neuroimage.2011.06.018

Zhou, J., Greicius, M. D., Gennatas, E. D., Growdon, M. E., Jang, J. Y., Rabinovici, G. D., … Seeley, W. W. (2010). Divergent network connectivity changes in behavioural variant frontotemporal dementia and Alzheimer's disease. *Brain*, *133*(Pt 5), 1352–1367. https://doi.org/10.1093/brain/awq075

SUPPORTING INFORMATION

Additional supporting information may be found online in the Supporting Information section.

Figure S1. Distribution of the normal component of the E-field (E_n in units of V/m) in the cortical surface. The top row shows the E-field induced by the bipolar montage, whereas the bottom one shows the E-field induced by the multichannel montage (anodes in red, cathodes in blue). The inset in figure 1b shows the mask of the motor cortex representation of the hand area in the left hemisphere

Figure S2. ICA components extracted from subjects' resting data, representing sensorimotor (SMN), visual (VN), left and right frontoparietal control (FPCN), auditory (AN), posterior default mode (pDMN), dorsal attention (DAN) and anterior default mode network (aDMN)

Figure S3. Effect of bifocal tDCS on network-to-network connectivity. The results of ANOVA conducted including the factor Condition (active, sham), Time (baseline, acute, cumulative, after), and the interaction Condition × Time, confirmed our hypothesis of no effectiveness of bifocal tDCS on negative correlated nodes to SMN. No significant effect of Condition ($F_{(1,9)} = 0.26$; $p = 0.62$), Time ($F_{(3,27)} = 0.18$; $p = 0.19$) and of Condition × Time interaction ($F_{(3,27)} = 1.54$; $p = 0.23$) has been reported

Table S1. ICA connectivity results. MNI coordinates, cluster size and localization of significant clusters displaying increased connectivity for net-tDCS compared to bifocal tDCS, both during and after stimulation.

Table S2. Mean and Standard Deviation (SD) for each subjective sensation reported trough a self-report questionnaire by conditions and montages

Transparent Peer Review Report

Transparent Science Questionnaire for Authors

How to cite this article: Mencarelli L, Menardi A, Neri F, et al. Impact of network-targeted multichannel transcranial direct current stimulation on intrinsic and network-to-network functional connectivity. *J Neurosci Res*. 2020;98:1843–1856. https://doi.org/10.1002/jnr.24690